Acta Crystallographica Section D
Biological Crystallography
ISSN 0907-4449

The role of substrate-binding groups in the mechanism of aspartate-β-semialdehyde dehydrogenase

Julio Blanco, Roger A. Moore,‡ Christopher R. Faehnle, David M. Coe and Ronald E. Viola*

Department of Chemistry, University of Toledo, Toledo, Ohio 43606, USA

‡ Present address: Laboratory of Persistent Viral Diseases, Rocky Mountain Laboratories, NIAID, NIH, Hamilton, MT 59840, USA.

Correspondence e-mail: ron.viola@utoledo.edu

Received 24 May 2004
Accepted 28 May 2004

PDB References: R270K ASADH, 1ps8, r1ps8sf; E243D ASADH, 1q2x, r1q2xsf; R103L ASADH, 1oza, r1ozasf; R103K ASADH, 1pr3, r1pr3sf; K246R ASADH, 1pu2, r1pu2sf.

The reversible dephosphorylation of β-aspartyl phosphate to L-aspartate-β-semialdehyde (ASA) in the aspartate biosynthetic pathway is catalyzed by aspartate-β-semialdehyde dehydrogenase (ASADH). The product of this reaction is a key intermediate in the biosynthesis of diaminopimelic acid, an integral component of bacterial cell walls and a metabolic precursor of lysine and also a precursor in the biosynthesis of threonine, isoleucine and methionine. The structures of selected *Haemophilus influenzae* ASADH mutants were determined in order to evaluate the residues that are proposed to interact with the substrates ASA or phosphate. The substrate K_m values are not altered by replacement of either an active-site arginine (Arg270) with a lysine or a putative phosphate-binding group (Lys246) with an arginine. However, the interaction of phosphate with the enzyme is adversely affected by replacement of Arg103 with lysine and is significantly altered when a neutral leucine is substituted at this position. A conservative Glu243 to aspartate mutant does not alter either ASA or phosphate binding, but instead results in an eightfold increase in the K_m for the coenzyme NADP. Each of the mutations is shown to cause specific subtle active-site structural alterations and each of these changes results in decreases in catalytic efficiency ranging from significant (~3% native activity) to substantial (<0.1% native activity).

1. Introduction

Following the aspartokinase-catalyzed activation of the β-carboxyl group of aspartic acid, aspartate-β-semialdehyde dehydrogenase (ASADH) uses an active-site cysteine nucleophile to catalyze dephosphorylation of the β-aspartyl phosphate (βAP) product to L-aspartate-β-semialdehyde (ASA) (Fig. 1). This metabolite occupies the first branch point in the pathway that ultimately leads to the synthesis of lysine, methionine, threonine and isoleucine (Cohen, 1983; Viola, 2001). The aspartate biosynthetic pathway is absent in eukaryotic organisms, raising interest in the design of selective inhibitors of these enzymes as potential antimicrobials. This aspartate pathway is also found in plants and an improved understanding of the regulation of this pathway could potentially alter the flux and increase the yields of essential amino

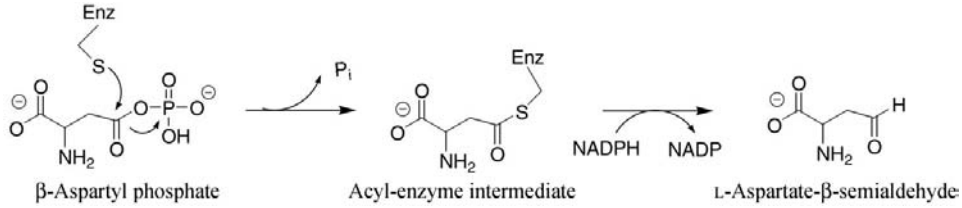

Figure 1
An abbreviated mechanism of the reaction catalyzed by aspartate β-semialdehyde dehydrogenase.

acids in plants. Several bacterial ASADHs have been purified and structurally characterized (Blanco, Moore, Kalabeeswaran *et al.*, 2003; Blanco, Moore & Viola, 2003; Hadfield *et al.*, 1999, 2001) and the first plant ASADH was recently purified from *Arabidopsis* (Paris *et al.*, 2002). Despite having only 26% overall sequence identity to the *Escherichia coli* enzyme, the *Arabidopsis* ASADH contains the same critical active-site functional groups as the microbial members of this enzyme family.

A family of functionally related enzymes from different organisms may possess only subtle differences in their ability to interact with substrates, substrate analogs and inhibitors. Once identified, exploiting these differences has the potential to lead to the development of highly specific antimicrobials designed to combat infectious drug-resistant organisms. At present, there are not enough well characterized examples of ASADHs from different organisms to evaluate how substrate specificity and binding recognition might vary in this enzyme family. We have recently examined the function of the cysteine–histidine dyad in the catalytic cycle of ASADH from *Haemophilus influenzae* (Blanco *et al.*, 2004). In this paper, we report kinetic, thermodynamic and structural characterization of selected mutants of *H. influenzae* ASADH (*hi*ASADH), focusing on those active-site groups that are proposed to function in the binding and selectivity of the substrates ASA (Arg270, Glu243) and phosphate (Arg103, Lys246).

2. Experimental procedures

2.1. Preparation and purification of ASADH mutants

The *asd* gene from *H. influenzae* that encodes ASADH was subcloned into a pET expression system (pET41a/*asd*) and overexpressed as described previously (Moore *et al.*, 2002). Mutations were created with this vector as the template using the QuikChange protocol (Strategene). Each mutant enzyme was purified to homogeneity through slight alterations in the protocol that has been used for purification of the native enzyme (Moore *et al.*, 2002).

2.2. DNA sequencing

Gene inserts were first characterized by restriction mapping and were then verified by forward and reverse sequencing of the plasmid DNA using T7 primers by the fluorescent dideoxy-terminator method using an ABI 3100 capillary sequencer (ACTG Inc., Northbrook, IL, USA).

2.3. Crystallization of the mutant apoenzymes

The mutant enzymes were concentrated by ultrafiltration (Millipore) to >10 mg ml^{-1} and dialyzed against 10 m*M* Na HEPES pH 7.0 containing 1 m*M* EDTA and 1 m*M* DTT. Crystallization conditions were obtained by hanging-drop vapor diffusion through optimizing the initial conditions obtained using the PEG/Ion Screen (Hampton Research). Crystals of the ASADH-binding mutants were grown at 293 K in 1:1 mixtures of enzyme and precipitant solution; diffraction-quality crystals were obtained with 22–24% PEG 3350 as the precipitant in the presence of 0.2 *M* ammonium acetate.

Table 1
Data-collection statistics for the *H. influenzae* ASADH-binding mutants.

Values in parentheses are for the highest resolution shell.

Data set	R270K	E243D/ ASA	R103L	R103K/ P_i	K246R/ ASA
Wavelength (Å)	1.00	1.00	1.00	1.54	1.00
Space group	$P2_12_12$	$P2_1$	$P2_12_12$	$P2_12_12$	$P2_12_12$
Unit-cell parameters					
a (Å)	113.8	54.6	112.7	114.2	113.8
b (Å)	54.6	113.9	53.9	54.9	54.7
c (Å)	57.1	57.3	55.1	58.3	57.2
β (°)		90			
Resolution limit (Å)	2.4	2.05	2.06	2.15	2.06
No. observations					
Measured	554823	460492	356150	149666	269874
Unique	14390	42991	21355	22055	27766
Completeness (%)	99.4 (100)	97.5 (94.5)	99.8 (100)	98.0 (98.0)	95.5 (96.8)
R_{sym}† (%)	8.8 (26.8)	5.5 (24.0)	8.9 (32.5)	6.2 (20.5)	5.5 (17.6)
Average $\langle I/\sigma(I)\rangle$	21.6 (5.8)	19.1 (5.6)	40.6 (6.6)	28.0 (7.8)	31.7 (10.0)

† $R_{sym} = \sum_{hkl}\sum_i |I_{hkl,i} - \langle I_{hkl}\rangle| / \sum_{hkl,i} I_{hkl,i}$, where $I_{hkl,i}$ is the intensity of an individual measurement of the reflection with Miller indices *hkl* and $\langle I_{hkl}\rangle$ is the mean intensity of that reflection.

2.4. Formation of enzyme–substrate complexes

The apoenzyme crystals were complexed by soaking with either ASA or phosphate. ASA was added to the mother liquor from a stock concentration of 100 m*M* to a final concentration of 2 m*M*. For soaks with the R103L mutant, sodium phosphate was included at a final concentration of 100 m*M*. The crystals were soaked in this solution for 1 h prior to harvesting. A harvesting solution was prepared (26% PEG 3350, 0.2 *M* ammonium acetate, 2 m*M* ASA or 100 m*M* phosphate and 0.1 *M* Tris–HCl pH 8.5 containing 20% glycerol) and this solution was introduced stepwise over approximately 1 h in order to minimize damage to the crystals, which were subsequently flash-frozen for X-ray diffraction data collection.

2.5. Data collection and processing

Diffraction data from crystals of the R103K complex with phosphate were collected on a rotating-anode home source equipped with an R-AXIS IV detector (detector distance 160 mm; 1° oscillation per image). A complete data set was collected from a single frozen crystal of R103L ASADH mutant on a Quantum-210 imaging plate (detector distance 200 mm; 1° oscillation per image) at the IMCA-CAT beamline (17-ID) at Argonne National Laboratory (APS). Diffraction data for the remainder of the mutants were collected at the Structural Biology Center (SBC) beamline at APS using a SBC-2 CCD X-ray detector. The images from each detector were processed and scaled using the program *HKL*2000 (Otwinowski & Minor, 1997). Data-collection statistics for each of these data sets are summarized in Table 1.

Table 2
Structural refinement statistics for the ASADH-binding mutants.

	R270K	E243D/ ASA	R103L	R103K/ P_i	K246R/ ASA
Refinement					
Resolution range (Å)	50–2.40	50–2.05	50–2.06	50–2.15	50–2.06
R_{cryst} (%)	22.2	23.8	20.8	22.2	23.6
R_{free} (%)	28.5	27.9	24.3	27.7	28.8
No. protein atoms	2752	5506	2749	2751	2756
No. non-protein atoms	0	16	0	5	8
No. water molecules	59	212	134	143	133
Stereochemistry					
R.m.s.d. for bond lengths (Å)	0.006	0.013	0.005	0.006	0.012
R.m.s.d for bond angles (°)	1.4	1.7	1.3	1.3	1.7
Residues in the Ramachandran plot					
Most favored region (%)	85.7	91.1	89.6	90.9	90.6
Additional allowed regions (%)	13.3	8.4	9.4	8.4	9.1
Generously allowed regions (%)	1.0	0.5	1.0	0.6	0.3

2.6. Structure solution and refinement

Data sets from the ASADH-binding mutants belong to the $P2_12_12$ space group and give a monomer in the asymmetric unit, except for the E243D mutant, which was solved as a dimer in space group $P2_1$. All mutant structures were solved by molecular replacement using a subunit of *H. influenzae* apo-ASADH (PDB code 1nwc) as the search model. The *CNS* package (Brünger *et al.*, 1998) was used for the rotation and translation searches. Rigid-body refinement led to an *R* factor of approximately 30% in the resolution range 20.0–3.0 Å. Simulated-annealing refinement at 2.5 Å was applied to the coordinate file obtained from the rigid-body refinement in order to improve the *R* factor. Model building was applied using *XtalView* (McRee, 1999). Several iterations of refinement and model building improved the final structures. The refined coordinates have each been deposited with the PDB, with the final refinement statistics listed in Table 2.

2.7. Kinetic studies

Enzyme assays were performed by measuring the initial rates in the reverse biological direction (Moore *et al.*, 2002). The data were fitted to an enzyme-kinetics software package adapted from earlier kinetics programs (Cleland, 1967). Protein concentrations were determined by comparison with standard curves using the method of Bradford (1976).

2.8. Differential scanning calorimetry

The *hi*ASADH wild-type and mutant enzymes were dialyzed against 50 m*M* Na HEPES pH 8.5, 0.5 m*M* TCEP and concentrated to 37 µ*M*. Solutions were degassed for 10 min before being loaded into their respective sample and reference cells in a VP-Differential Scanning Calorimeter (MicroCal Inc., Amherst, MA, USA). A stable reference baseline was established before sample analysis. The protein samples were scanned relative to the buffer/TCEP reference solution over a temperature range of 298–353 K at a scan rate of 90 K h^{-1}, with data points taken every 16 s. Data analysis was performed by subtracting reference data from the sample data and normalized by concentration using the *Origin* software package (OriginLab Corp., Northampton, MA, USA). The deconvolution of unfolding endotherms was prepared with the *Origin* peak-fitting module using a non-two-state fitting parameter.

3. Results and discussion

The ASADHs from a variety of organisms encompass a considerable diversity of sequence homologies, ranging from as little as 10% to as high as 95% sequence identity to the *E. coli* enzyme. Despite this sequence diversity, the identity of the core active-site functional groups have been preserved throughout evolution. We have examined a set of active-site mutants of ASADH from *H. influenzae* with the goal of more precisely establishing the role of each functional group in substrate recognition and binding.

3.1. An important substrate-binding group

A conserved arginine (Arg270) in the ASADH family aligns with Arg231 in glyceraldehyde-3-phosphate dehydrogenase (GAPDH), a residue that has been assigned a role in binding the substrate phosphate group (Skarzynski *et al.*, 1987). Based on kinetic studies (Ouyang & Viola, 1995), this arginine residue was proposed to have a comparable role in *hi*ASADH, namely binding the carboxyl group of the substrate ASA. The structures of complexes of native enzyme, both as a hemithioacetal intermediate (Blanco, Moore & Viola, 2003) and with the inactivator *S*-methyl-L-cysteine sulfoxide (SMCS) covalently bound to *Vibrio cholerae* ASADH (Blanco, Moore, Kalabeeswaran *et al.*, 2003), have now clearly established the presence of a bidentate interaction between Arg270 and the carboxylic group of the substrate ASA. This interaction appears to be required to orient the tetrahedral hemithioacetal intermediate that is formed from ASA during the catalytic cycle. Maintaining this orientation is important for the subsequent hydride transfer to NADP, thereby forming the thioester intermediate as the next step in the catalytic cycle examined in the reverse biological direction (Blanco, Moore & Viola, 2003). Arg270 was replaced by lysine in *hi*ASADH in order to assess its relative importance in substrate binding by disrupting the bidentate interaction that is formed with ASA and the catalytic intermediates.

Only poorly diffracting crystals were obtained when the R270K mutant was either cocrystallized or soaked in the presence of various combinations of substrates. The highest resolution R270K structure was solved in the absence of substrates or coenzyme and shows clear electron density for the lysine moiety that replaces Arg270. Comparison of the native enzyme structure with that of R270K shows that the ε-amino group of this lysine is positioned 1.7 Å away from the location of the closest terminal guanidino N atom of Arg270. The reorientation of the Arg270 side chain that takes place during formation of the hemithioacetal intermediate (Blanco, Moore & Viola, 2003) would further increase the distance between the position of the Arg270 guanidino group and the position occupied by the lysine amino group in the R270K

Table 3
Kinetic parameters of *H. influenzae* ASADH-binding mutants.

		ASA		Phosphate		NADP	
Enzyme	k_{cat} (s^{-1})	K_m (mM)	k_{cat}/K_m (M^{-1} s^{-1})	K_m (mM)	k_{cat}/K_m (M^{-1} s^{-1})	K_m (mM)	k_{cat}/K_m (M^{-1} s^{-1})
Native	330 ± 17	0.20 ± 0.03	1.4×10^6	1.6 ± 0.2	2.1×10^5	0.20 ± 0.03	2.2×10^6
R270K	0.4 ± 0.03	0.40 ± 0.06	1.0×10^3	1.9 ± 0.3	2.1×10^2	0.17 ± 0.03	2.4×10^3
E243D	4.0 ± 0.2	0.20 ± 0.02	3.6×10^4	1.5 ± 0.2	4.0×10^3	1.6 ± 0.2	4.0×10^3
R103K	1.2 ± 0.1	0.10 ± 0.02	9.1×10^3	36.6 ± 5.1	3.3×10^1	0.7 ± 0.1	1.0×10^3
R103L	0.24 ± 0.01	0.030 ± 0.004	8.0×10^3	240 ± 67	1.0×10^0	0.11 ± 0.02	2.2×10^4
K246R	11.0 ± 1.0	0.10 ± 0.03	1.1×10^5	1.0 ± 0.2	1.1×10^4	0.60 ± 0.08	1.0×10^4

apoenzyme structure. If the lysyl side chain of the R270K fails to respond to this repositioning, then this would leave the ε-amino nitrogen of Lys270 more than 5 Å away from the carboxylic group in the intermediate structure (Fig. 2).

Previous kinetic studies showed that R267L *ec*ASADH (analogous to Arg270 *hi*ASADH) retains about 10% of the native activity, but the K_m for ASA and phosphate in this *E. coli* mutant increase by factors of 31 and 4, respectively (Ouyang & Viola, 1995). In contrast, in the more conservative *hi*ASADH R270K mutant the K_m for ASA only increases by a factor of two. However, the k_{cat} value of the R270K mutant is only about 0.1% of that of the native enzyme (Table 3), a nearly 100-fold greater activity loss in this *H. influenzae* mutant than in the *E. coli* mutant, which is more drastically altered at this same position. A comparison of these kinetic data suggest that the introduced lysine in *hi*ASADH R270K must be capable of an initial interaction with the carboxylic group of the substrate, since no significant change is observed in the K_m of ASA for this mutant compared with the native enzyme. Maintaining this interaction between Lys270 and the intermediate carboxyl group would require a shift in the orientation of both the lysyl side chain and the tetrahedral intermediate relative to their positions in the native enzyme. The dramatic loss of activity in R270K can potentially be explained by the movement of the intermediate that would be necessary to form and maintain a suitable interaction between the intermediate carboxyl group and the mutated substrate-binding group during the catalytic cycle. The neutral side chain introduced in *ec*ASADH R267L cannot interact with the substrate carboxyl group, leading to a substantial increase in the K_m for ASA, but at the same time allowing greater conformational flexibility for the covalent intermediate. This flexibility would increase the likelihood that the intermediate could adopt a catalytically viable conformation relative to that imposed in *hi*ASADH R270K, consistent with the 100-fold greater activity seen in R267L *ec*ASADH.

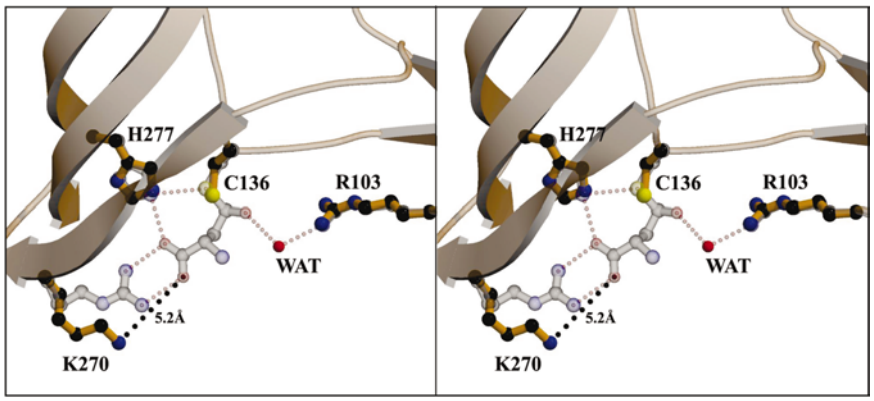

Figure 2
Stereoview of an overlay of the native ASADH intermediate structure (gray) and the R270K mutant structure (orange). The shift in the position of Lys270 in the apoenzyme is compared with the position of the arginine at this position in the intermediate complex of the native enzyme.

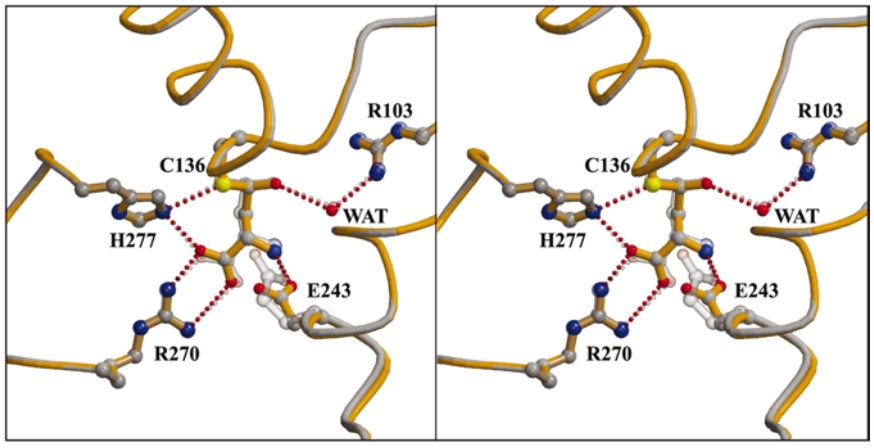

Figure 3
Comparison of the active-site structures of the native ASADH intermediate structure (gray) and the E243D mutant (orange). The carboxyl side chain at position 243 and the α-amino group of the covalently bound intermediate have each reoriented to maintain hydrogen-bonding contact in the E243D mutant enzyme.

3.2. A substrate-orienting group

Glu243 provides a side-chain carboxyl group in the active site of ASADH whose role in the catalytic cycle has not been definitively established. This group is highly conserved among ASADHs from different organisms and we have shown that it is in

position to potentially interact with the amino group of the hemithioacetal intermediate in the *hi*ASADH complex (Blanco, Moore & Viola, 2003). In this study, Glu243 has been mutated to aspartate in order to assess its possible role in substrate and intermediate binding. Kinetic studies on the E243D mutant failed to show the expected detrimental effect on substrate interactions, with the K_m for ASA unchanged from that of the native enzyme (Table 3). Instead, the catalytic efficiency of this mutant is significantly compromised, reducing the k_{cat} value to about 1% of that of native *hi*ASADH.

The structure of E243D was solved in the presence of the substrate ASA in order to investigate the changes in the active site responsible for this loss of activity. The overall structure of this E243D–ASA complex does not deviate substantially from that of the corresponding native *hi*ASADH–ASA complex structure. The most significant changes occur at the site of mutation and in the orientation of the bound ASA. In each of the native enzyme structures that have been previously examined (Blanco, Moore, Kalabeeswaran *et al.*, 2003; Hadfield *et al.*, 2001), ASA (or the active site-directed inactivator SMCS) binds in an orientation that would facilitate a stereospecific nucleophilic attack by Cys136 on the substrate aldehydic carbon to form a covalently bound hemithioacetal intermediate with *R* stereochemistry (Blanco, Moore & Viola, 2003). Despite the low catalytic activity in the E243D mutant, formation of the same tetrahedral intermediate is observed. This mutant compensates for the shorter side-chain length at position 243 by reorienting the aspartate carboxyl group to locate it within 0.5 Å of the original glutamate carboxyl group position in the native enzyme. This reorientation serves to maintain the critical hydrogen-bonding interaction with the ASA amino group (Fig. 3). However, the shorter length of Asp243 results in a displacement of the active-site loop (residues 232–245) away from the tetrahedral intermediate. To compensate for this backbone shift, the hemithioacetal group moves towards Asp243 by about 0.5 Å, while still maintaining its important hydrogen-bonding interactions with both Arg270 and His277 (Fig. 3). This movement leads to other subtle shifts within the active site. The average distance from the Arg270 guanidino group to the α-carboxyl O atoms of the bound intermediate increases by 0.3 Å and the distance between the water molecule bound in the phosphate site and the intermediate α-amino group increases by 0.2 Å. While each of these shifts alter enzyme–substrate interactions, none of the observed changes in the E243D structure appear to be sufficient by themselves to account for the significant loss of activity. However, completion of the catalytic cycle requires the formation of at least two additional enzyme intermediates, with corresponding side chain and intermediate movements expected, and the structures of these complexes have not been determined.

3.3. Role of a key phosphate-binding group

We have recently established that phosphate is engaged in a bidentate interaction with Arg103 that supports efficient catalysis (Blanco, Moore & Viola, 2003). This critical electrostatic contact positions the phosphate group to interact with both the hemithioacetal oxygen and the amino group of the tetrahedral intermediate formed from ASA, thereby optimizing its position for subsequent nucleophilic attack on the thioester intermediate. In this study, Arg103 was mutated to both lysine and leucine in order to investigate the relative importance of this active-site residue in supporting the ASADH-catalyzed reaction. The ability of either of these Arg103 mutants to catalyze the conversion of ASA to aspartyl-phosphate is severely impaired, with residual activities of 0.4 and 0.07%, respectively, relative to the native

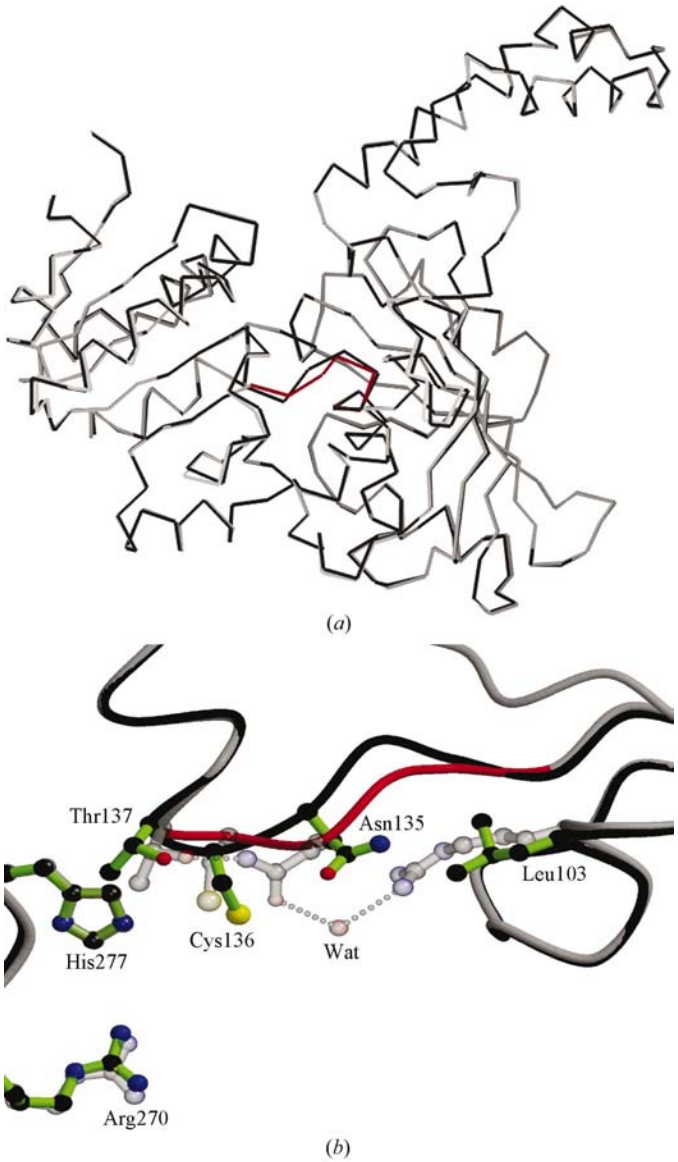

Figure 4
Overlay of the backbone drawings of native (light) and R103L mutant (dark) *hi*ASADH structures. (*a*) The overall fold and backbone position of the native and mutant structures are essentially the same, except for the reorientation of a critical active-site loop (shown in red). (*b*) Disruption of the water-mediated hydrogen-bonding network between Arg103 and Asn135 in the R103L mutant that triggers this loop movement and shifts the position of the active-site Cys136 nucleophile. The calculation for the overlay was performed with *XtalView* and the drawing was produced using *SPOCK*.

enzyme (Table 3). In addition, unlike the other binding groups that were mutated, alterations at Arg103 have a direct impact on phosphate binding. Substitution with lysine at this position results in a nearly 25-fold increase in K_m and replacement with a neutral leucine leads to a 150-fold increase in phosphate K_m (Table 3).

High-resolution structures of the R103L and R103K mutants were determined in order to provide an explanation for the loss of catalytic activity and substrate binding. The overall structure of the R103L mutant is essentially the same as that of the native enzyme, with the exception of an active-site loop (Asn135–Ser139) that has shifted with respect to its original position in the native enzyme (Fig. 4*a*). Rearrangement of this loop can be attributed to the loss of key hydrogen bonds between the ASA-binding residues and Arg103 that are now disrupted in R103L. The native enzyme will accommodate either a phosphate or a water molecule in this binding pocket and interactions with these bound ligands play a critical role in stabilizing the tetrahedral intermediate formed by attack of Cys136 on ASA (Blanco, Moore & Viola, 2003). However, the expected water molecule is not observed at this position in the R103L structure (Fig. 4*b*). Its absence prevents the formation of a hydrogen-bonding network that is present in the native enzyme between the amide side chain of Asn135, the water molecule and the guanidino group of Arg103. The shift of this loop (Asn135–Ser139) as a consequence of the loss of these stabilizing hydrogen bonds disrupts the fine-tuned catalytic machinery of ASADH. The position of the active-site thiol of Cys136 moves nearly 1 Å further away from the N^{ε} atom of its catalytic partner, His277, effectively putting it out of range for proton transfer and for stabilization of the acyl-enzyme intermediate that is formed at this cysteine. This loop movement also shifts the peptide amide group of Asn135 out of position so that it can no longer stabilize the developing negative charge on the O atom of the hemithioacetal intermediate (Blanco, Moore & Viola, 2003). Disruption of the phosphate-binding site also raises the level of phosphate required to fully occupy this site, essentially decreasing the effective nucleophile concentration in the active site of the enzyme. Thus, the replacement of one hydrogen-bonding partner by an active-site water molecule, as well as a binding partner for phosphate, disrupts a network of hydrogen bonds that has drastic consequences for catalysis.

To minimize the perturbation at this position Arg103 was also mutated to lysine, a functional group with the potential to form only a monodentate interaction with phosphate. This mutant structure displays clear electron density for the mobile Asn135–Ser139 active-site loop and the backbone folding in this particular region is the same as that of the native enzyme (Fig. 5). The side chain of Lys103 adopts a similar position to that of the native arginine. However, despite extensive incubation in the presence of excess phosphate, a water molecule is observed at this binding site in place of the expected phosphate. A phosphate ion is found in the R103K structure, but it is bound at a nonproductive ancillary site that was previously identified in the *hi*ASADH tetrahedral intermediate structure (Blanco, Moore & Viola, 2003). The bound phosphate at this adjacent site does not have direct contact with ASA and is unlikely to play a role in catalysis. This second phosphate site is within hydrogen-bonding distance of the substrate phosphate position in the intermediate structure as well as to Lys246, while engaging in additional interactions with Glu232, Lys242 and Ser100. As with the native enzyme, the binding of this ancillary phosphate is not involved in the catalytic mechanism and is likely to be an artifact of the high phosphate levels present in the soaking and harvesting conditions. The improved orientation of Asn135 results in a sixfold decrease in phosphate K_m and a fivefold increase in catalysis relative to the R103L mutant. However, the inability to provide a bidentate binding partner to phosphate at position 103 still leads to a significantly impaired catalyst.

3.4. A phosphate-orienting group

Lys246 in the native *hi*ASADH interacts with the bound phosphate in the hemithioacetal intermediate structure (Blanco, Moore & Viola, 2003). As with Arg103, this functional group is ideally positioned to orient the phosphate for nucleophilic attack on the carbonyl group of the thioester intermediate. Lys246 was mutated to arginine, a residue than can potentially increase the number of interactions with phosphate. However, instead of an improvement in the ability of the K246R mutant to interact with phosphate, the K_m for phosphate is essentially unchanged in this mutant. Instead, the k_{cat} of K246R decreases to only 3% of the native enzyme (Table 3).

The K246R structure was determined as a binary complex with ASA in order to explore the reasons for this loss of activity. Well defined density is observed in the active site for both Arg246 and for the tetrahedral intermediate that is formed by attack of Cys136 on ASA. The intermediate in this mutant enzyme is positioned virtually identically to the orientation observed in the native *hi*ASADH–ASA complex structure (Blanco, Moore & Viola, 2003). The

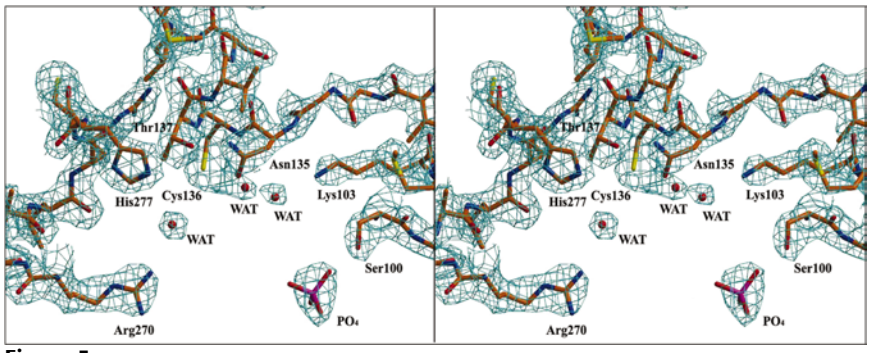

Figure 5
Stereoview of the electron density at the active site of the *hi*ASADH R103K mutant showing the position of Lys103 and the presence of a water molecule (adjacent to this lysine) in place of phosphate in the phosphate-binding site. Phosphate is found only at an ancillary site that had previously been detected (Blanco, Moore & Viola, 2003).

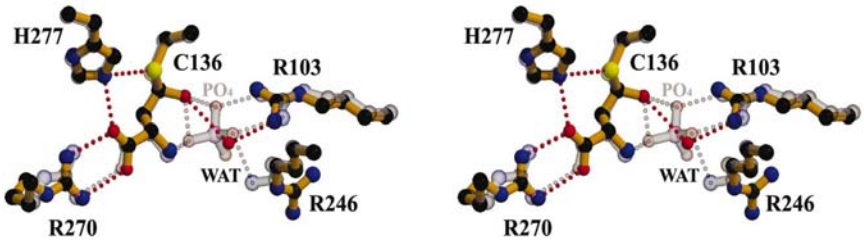

Figure 6
Stereoview of an overlay of the native ASADH intermediate complex with phosphate (gray) and the K246R intermediate structure (orange). While the positions of the other active-site residues are unchanged, the introduced arginine (Arg270) has moved out of the phosphate-binding site. Rotation of the guanidino group would be needed to bring this functional group into position to interact with a bound phosphate.

Table 4
Thermal stability of ASADH mutants.

Sample	T_m (K)
Native	333.7 ± 0.4
R270K	332.3 ± 0.3
C136S	332.4 ± 0.3
R103L†	326.3 ± 0.1
R103K	326.9 ± 0.7
E243D	325.5 ± 0.2
H277N	337.3 ± 0.3
K246R	337.5 ± 0.3

† A second, weaker thermal transition is observed for this mutant at 332.5 K.

positions of the active-site residues are also essentially the same and only small changes are observed in the positions of the backbone atoms near the site of mutation. The Arg246 side chain folds into the same position as that of the native lysine, except that the terminal N atoms of the guanidino group are now rotated by about 90° relative to that of the lysine ε-amino group (Fig. 6) and make new interactions with the side chains of Ser100 and Lys242. This new orientation places the N^{ε} of Arg246 about 4 Å away from the position of the catalytic phosphate. This distance is too great for any direct interactions that could help to orient and stabilize this oxyanion and would require a rotation of this arginyl side chain in order to bring the guanidino group into position to act as a binding ligand for phosphate. Thus, instead of providing an additional ligand to bind and position the phosphate, the substitution of an arginine for Lys246 has a detrimental effect on the integrity of this site.

3.5. Stability of the ASADH mutants

The impaired ability of a mutant enzyme to catalyze a reaction can be a consequence not only of structural alterations, but may also be the result of a decrease in enzyme stability. A recent study examined a set of adenylosuccinate lyase mutants at positions that were implicated in this enzyme deficiency in humans (Palenchar *et al.*, 2003). Surprisingly, the kinetic parameters of these mutants were essentially unchanged from those of the native enzyme; however, these enzyme variants were found to have marked thermal instability. To examine this possibility in ASADH, the thermal transition temperature (T_m) was determined by differential scanning calorimetry for each of the mutants and compared with the value for the native enzyme. The T_m of the catalytic C136S mutant is unchanged from that of the native enzyme, while the H277N mutant is slightly more stable (Table 4). Most of the binding mutants that have been prepared have either similar or slightly enhanced thermal stability relative to the native enzyme. The E243D mutant that has an altered interaction with ASA has a T_m that is 8 K lower and the Arg103 mutants with altered phosphate-binding affinity are less stable than the native enzyme by about 7 K. The stability of the R103K mutant was examined in the presence of phosphate in order to reproduce the crystallization conditions of the binary complex and to determine whether phosphate binding will stabilize this mutant. The T_m for the R103K–P_i complex does increase by over 6 K to a value (333.2 K) that is nearly identical to that of the native enzyme. However, phosphate binding also further stabilizes the native enzyme, increasing the T_m by nearly 4 K. While these changes in stability between the native enzyme and several mutants are significant, they are not by themselves sufficient to account for the diminished catalytic activity observed in these mutants.

4. Conclusions

Each of these mutations was prepared with the aim of removing critical substrate-binding groups. Replacement of Arg103 does result in a dramatic elevation in the K_m of phosphate. For the remaining mutants, the structural rearrangements that occur as a consequence of these replacements manifest themselves not in a loss in substrate-binding affinity, but in a loss of catalytic activity. Structural characterization of these mutants show that in each case only subtle changes in key active-site residues, rotation of a side chain to form a new hydrogen bond or a shift in position relative to a catalytic intermediate are sufficient to adversely affect catalysis.

The authors wish to thank Dr Tim Mueser for helpful discussions on the analysis and refinement of the enzyme structures and the *E. coli* Genetic Stock Center (Yale University) for providing the *asd*-deficient cell line. Use of the Argonne National Laboratory at the Advanced Photon Source was supported by the US Department of Energy, Office of Energy Research under Contract No. W-31-109-ENG-38. We thank the staff members at the Structural Biology Center (SBC) and IMCA-CAT for their assistance with data collection.

References

Blanco, J., Moore, R. A., Faehnle, C. R. & Viola, R. E. (2004). In the press.

Blanco, J., Moore, R. A., Kalabeeswaran, V. & Viola, R. E. (2003). *Protein Sci.* **12**, 27–33.
Blanco, J., Moore, R. A. & Viola, R. E. (2003). *Proc. Natl Acad. Sci. USA*, **100**, 12613–12617.
Bradford, M. (1976). *Anal. Biochem.* **72**, 248–253.
Brünger, A. T., Adams, P. D., Clore, G. M., DeLano, W. L., Gros, P., Grosse-Kunstleve, R. W., Jiang, J.-S., Kuszewski, J., Nilges, M., Pannu, N. S., Read, R. J., Rice, L. M., Simonson, T. & Warren, G. L. (1998). *Acta Cryst.* D**54**, 905–921.
Cleland, W. W. (1967). *Adv. Enzymol.* **29**, 1–32.
Cohen, G. N. (1983). *Amino Acids: Biosynthesis and Genetic Regulation*, edited by K. M. Herrmann & R. L. Somerville, pp. 147–171. Reading, MA, USA: Addison–Wesley.
Hadfield, A. T., Kryger, G., Ouyang, J., Petsko, G. A., Ringe, D. & Viola, R. E. (1999). *J. Mol. Biol.* **289**, 991–1002.
Hadfield, A. T., Shammas, C., Kryger, G., Ringe, D., Petsko, G. A., Ouyang, J. & Viola, R. E. (2001). *Biochemistry*, **40**, 14475–14483.
McRee, D. E. (1999). *J. Struct. Biol.* **125**, 156–165.
Moore, R. A., Bocik, W. E. & Viola, R. E. (2002). *Protein Expr. Purif.* **25**, 189–194.
Otwinowski, Z. & Minor, W. (1997). *Methods Enzymol.* **276**, 307–326.
Ouyang, J. & Viola, R. E. (1995). *Biochemistry*, **34**, 6394–6399.
Palenchar, J. B., Crocco, J. M. & Colman, R. F. (2003). *Protein Sci.* **12**, 1694–1705.
Paris, S., Wessel, P. M. & Dumas, R. (2002). *Protein Expr. Purif.* **24**, 99–104.
Skarzynski, T., Moody, P. C. & Wonacott, A. J. (1987). *J. Mol. Biol.* **193**, 171–187.
Viola, R. E. (2001). *Acc. Chem. Res.* **34**, 339–349.